Detection of Influenza Virus Using Peroxidase-mimic of Gold Nanoparticles

Detection of Influenza Virus Using Peroxidase-mimic of Gold Nanoparticles

Syed Rahin Ahmed,[1] Jeonghyo Kim,[2] Tetsuro Suzuki,[3] Jaebeom Lee,[2,*] and Enoch Y. Park[1,4,*]

[1] Research Institute of Green Science and Technology, Shizuoka University, 836 Ohya Suruga- ku, Shizuoka, 422-8529, Japan.

[2] Department of Cogno-Mechatronics Engineering, Pusan National University, Busan, 609-735, Republic of Korea.

[3] Department of Infectious Diseases, Hamamatsu University School of Medicine, 1-20-1 Higashi-ku, Handa-yama, Hamamatsu 431-3192, Japan.

[4] Graduate School of Science and Technology, Shizuoka University, 836 Ohya Suruga-ku, Shizuoka 422-8529, Japan.

E-mail: rahin_sust@yahoo.com (SRA)
yaamako@gmail.com (JK)
tesuzuki@hama-med.ac.jp (TS)
jaebeom@pusan.ac.kr (JL)
park.enoch@shizuoka.ac.jp (EYP)

[*]Correspondence to: Enoch Y. Park; J. Lee

ABSTRACT: A modified enzyme-linked immunosorbent assay (ELISA) with nanomaterials is an effective and powerful method to amplify the signal and reduce the cost of detecting and measuring trace biomarkers or proteins. In this study, an ultra-sensitive colorimetric immunoassay was designed, and its ability to detect influenza viruses using positively charged gold nanoparticles ((+)Au NPs) was assessed as a possible role for peroxidase-mimic inorganic enzymes. This method detected influenza virus A (H1N1) with a linear range up to 10 pg mL^{-1} and clinically isolated influenza virus A (H3N2) up to 10 plaque forming units (PFU) mL^{-1}, where its sensitivity improved to 500-fold higher than that of commercial virus kits. The sensitivity of this proposed method was not declined even though in complex biological media in compared to conventional ELISA. These results revealed that the (+)AuNP-based colorimetric immunoassay could be suitable for lab-on-a-chip device and open new opportunities for clinical protein diagnostics.

KEYWORDS: influenza virus; peroxidase-mimic enzymatic reaction; gold nanoparticles; immunoassay.

The importance of developing simple, sensitive, highly selective, and cost-effective bioassays for disease-related protein detection to control the spread of infectious viruses is increasing (Gao et al., 2014; Gubala et al., 2012; Rodríguez-Lorenzo et al., 2012). To date, various immunoassays for disease-related protein detection have been reported and developed, *e.g.*, surface plasmon resonance (Nguyen et al., 2015), metal-enhanced fluorescence (Ahmed et al., 2014), chemilluminescence (Khavan-Tafti et al., 2013), electrochemistry (Munge et al., 2013) and colorimetric methods (Gao et al., 2013). In particular, the enzymatic colorimetric method is used widely in immunoassays because of its simplicity, low cost, and easy readout (Gao et al., 2013; Perfezou et al., 2012). Many efforts have been devoted to using native enzyme labels as signal amplification strategies, e.g., horseradish peroxidase (HRP) (Lin et al., 2013), alkaline phosphatase (Jiang et al., 2013) and β-galactosidase (Hossain and Brennan, 2011). Unfortunately, the majority of the developed colorimetric immunoassays usually involve poor sensitivity due to limited signal amplification strategies or the requirement of a multi-step pre-treatment (Malashikhina et al., 2013). The preparation, purification and storage of natural enzymes are usually time-consuming, expensive and complicated, especially for enzymes functionalized with other biomolecules; therefore, their bioactivity may have adverse effects during the process (Gao et al., 2013).

Some nanomaterials possess enzyme-like activity. For example, Gao et al. (2013) has reported irregular-shaped platinum nanoparticles (NPs) that were utilized as peroxidase-like mimics for the development of colorimetric immunoassays. $ZnFe_2O_4$ magnetic NPs (Su et al., 2012) and graphene oxide-Fe_3O_4 magnetic nanocomposites (Dong et al., 2012) also have peroxidase-like activity and are used for colorimetric detection of glucose. However, most of the reported nanomaterials that show enzyme-

like activity are not easy to prepare; therefore, the development of easy-to-use methods of highly sensitive biosensors in the field of clinical diagnostics and medical treatment is needed. In particular, Au NPs can be used in a peroxidase-mimic enzymatic reaction and are a unique material that is easy to prepare. Furthermore, Au NPs allow easy tagging of the NPs with various proteins and biomolecules, and their high catalytic activity emerges at significantly reduced particle sizes. In particular, positively-charged Au NPs ((+)Au NPs) catalyze the oxidation of the peroxidase substrate 3,3',5,5'- tetramethylbenzidine (TMB) by H_2O_2 to develop a blue color in aqueous solution. Although a detailed biological mechanism has not been clearly revealed, a possible reason is related to the decomposition of the O-O bond of H_2O_2 to an HO• radical and further stabilization on the (+)Au NP surface via partial electron exchange interactions that may enhance NP catalytic activity (Jv et al., 2010).

Here, a highly sensitive method for influenza virus detection involving (+)Au NPs conjugated with influenza virus-specific antibodies was developed, which is the first proof-of-concept attempt and practical application to monitor influenza viruses under peroxidase-mimic enzymatic reaction of NPs. The (+)Au NPs were used as replacements of HRPs to catalyze the H_2O_2-mediated oxidation of TMB to develop a colorimetric immunoassay in a 96-well polystyrene microtiter plates (Fig. 1A) and to explore a very simple, highly sensitive and point-of-care readable bioassay.

The absorbance spectra of the synthesized (+)AuNPs are shown in Figure 1B. The absorbance peak of the (+)Au NP solution was located at 526 nm and calculated concentration was 3.5×10^{-10} M. The surface charge of (+)Au NPs was +34.5 mV. Furthermore, transmission electron microscope revealed (+)Au NP with an average size of 35 nm (Fig. 1C).

Then, the conjugation of anti-hemagglutinin (HA) antibodies (Ab66189) with (+)Au NPs was confirmed with a nano-gold beads based ELISA test and zeta potential analysis. Higher optical density in the UV spectrum was observed with antibody-conjugated (+)Au NPs than with only (+)Au NPs (Fig. 2A), which indicated that (+)Au NPs were successfully conjugated with antibodies. The change of zeta potential value also indicates the successful conjugation of antibodies with (+)Au NPs (Table S1, supporting information). Citrate capped negatively charged gold nanoparticles, (-)Au NPs were synthesized based on previously reported (Jana et al., 2001) and its plasmonic peak located at 530 nm and concentration was 7.9×10^{-11} M. The average particles size of synthesized (-)Au NPs was 37 nm with surface charges of -35.9 mV (Fig. S1, Table S1, supporting information). Furthermore, citrate capped (–)Au NPs was conjugated with antibodies through amide bond using EDC/NHS chemistry and confirmed by ELISA and zeta potential analysis (Fig. S2, Table S1, supporting information). As shown in Fig. S2, higher optical density was found from antibodies conjugated (-)Au NPs in compared to only (-)Au NPs reflects antibodies successful conjugation with (-)Au NPs. Also, The surface charge changes of (-)Au NPs confirmed its binding with antibodies. Then, a feasibility study of peroxidase activity was carried out using antibodies conjugated (+)Au NPs and (–)Au NPs. As shown in Figure 2B, the optical density of the absorbance spectrum and the color of the solution with antibody-conjugated (+)Au NPs developed a deep blue color within a few seconds after the addition of TMB-H_2O_2 solution; however, the (–)Au NP solution or antibody alone did not show an immediate color change, and the eventual color was pale blue. The optical density of (+)Au NPs was approximately 7-fold higher than that of (-)Au NPs and only antibodies, which indicated that the catalytic oxidation of TMB with H_2O_2 in the presence of (+)Au NPs was much faster and stronger,

demonstrating the feasibility of developing a rapid and sensitive colorimetric nanobiosensor. Regarding (–)Au NPs, negatively charged HO• radical loosely bound to this nanoparticle, and the electron exchange interaction was very weak, which resulted in slow catalytic oxidation and pale blue color development. Also, a comparison study of catalytic activities revealed that (+)Au NPs showed higher catalytic activities in compare to HRP which is crucial to introduce nanomaterials to conventional ELISA method and increase its sensitivity(Fig.S3).

The strong peroxidase-like activity of (+)Au NPs was applied to monitor influenza viruses A/New Caledonia/20/1999 (H1N1). The selectivity of this detection system was assessed using 4 different mixing components: a) target viruses/specific antibody (HA Ab 66189)-conjugated (+)Au NPs/TMB-H_2O_2, b) target virus/non-specific antibody (anti H3N2 MAb antibody)-conjugated (+)Au NPs/TMB-H_2O_2, c) target virus/specific antibody (HA Ab 66189)-conjugated (+)Au NPs/H_2O_2, and d) target virus/specific antibody (HA Ab 66189)-conjugated (+)Au NPs/TMB. In the experiment with solution a), deep blue color developed in the presence of target viruses and its specific antibody conjugated-(+)Au NPs after the addition of TMB-H_2O_2 solution, and a strong characteristic absorption peak at 655 nm was also achieved (Fig. 3A). However, no characteristic peak was observed for the other mixtures (Fig. 3A). These results revealed that the proposed sensing method was highly specific and could cause color development in the presence of TMB and H_2O_2.

A series of quantitative analyses with influenza virus A/New Caledonia/20/1999 (H1N1) were carried out, where the absorbance intensities of the unique color of the developed solution corresponded logarithmically to the target virus concentration within a relatively wide range of 10 pg mL^{-1} to 10 μg mL^{-1} (Fig. 3B), and the limit of detection

(LOD) was calculated as 10.79 pg mL^{-1} based on standard deviation method (Apostol et al., 2009). However, no significant color developed in the case of BSA and the non-specific virus (data not shown).

A series of feasibility tests were also performed using a clinically isolated influenza virus A/Yokohama/110/2009 (H3N2) sample. These experiments were carried out as described above with influenza virus A/New Caledonia/20/1999 (H1N1) to monitor specificity and sensitivity. Anti-H3 antibody specificity and its binding with (+)Au NPs were confirmed using nano-gold bead ELISA. Figure 4A (blank bar chart) shows the specificity of the anti-influenza H3N2 HA MAb for influenza virus A/Yokohama/110/2009, where only the sample with the target influenza generated color, reflecting enhancement of absorbance intensity at the designated wavelength. In the case of anti-H1N1 HA Ab66189 and BSA, no significant absorbance was obtained, which reflects the specificity of anti-influenza H3N2 HA MAb for influenza virus A/Yokohama/110/2009. In addition, the binding of anti-influenza H3N2 HA MAb with (+)Au NPs was confirmed with higher absorbance compared with bare (+)Au NPs using ELISA (Fig. 4A, pattern bar chart). Then, different concentrations of influenza virus A/Yokohama/110/2009 were monitored to draw the linearity of the absorbance response, where the sensitivity of influenza virus A/Yokohama/110/2009 (H3N2) detection was observed within the range of 10 ~ 50,000 plaque forming units (PFU) mL^{-1} (Fig. 4B), and the limit of detection (LOD) was calculated as 11.62 PFU mL^{-1}.

Regarding the influenza virus A/Yokohama/110/2009 (H3N2), comparisons of sensing performance were performed with both a commercially available influenza diagnostic test rapid kit (ImunoAce Flu, TAUNS Lab. Inc., Numazu, Shizuoka, Japan) that we reported previously (Ahmed et al., 2014) and conventional ELISA (Fig. 4C). In

ELISA, detection linearly correlated with the concentrations of the virus, which reached 1000 PFU mL^{-1}. The present sensing system was 100-fold more sensitive than the conventional ELISA and 500-fold more sensitive than the commercial kit (Ahmed et al., 2014).

When a series of different concentrations of H3N2 viruses were prepared in human serum, the results were mostly similar to the above results except at high virus concentrations (Fig. 4D). The detected optical density of the H3N2 virus concentration was significantly low (50 PFU mL^{-1}), demonstrating the reliability of this detection method.

In summary, we have reported an enhanced colorimetric immunoassay for highly sensitive detection of influenza viruses using (+)Au NPs as the signal amplifier. Colorimetric assays employing the catalytic activity of (+)Au NPs detected up to 10.79 pg mL^{-1} level concentrations of target influenza virus A (H1N1) and clinically isolated influenza A (H3N2) up to 11.62 PFU mL^{-1} with a limited assistance of optical instrument. This new approach using (+)Au NPs is simple, highly sensitive and can complete the sensing process in a few minutes without any significant equipment or training overhead, and has great potential to be applicable for in situ point-of-care (POC) diagnosis.

Materials and Methods

Chemicals, Antibodies and Virus Samples

$HAuCl_4 \cdot 3H_2O$ and human serum (contained extremely complex biological matrices in dL i.e., iron 35–180μg, cholesterol 110–210mg, triglyceride 30–175mg, glucose 60–140mg, endotoxin level < 10EU, hemoglobin < 20mg) were obtained from Sigma–

Aldrich(St. Louis, MO, USA). N-(3-dimethylaminopropyl)-N´-ethylcarbodiimide (EDC) and *N*-hydroxy succinimide (NHS) were purchased from Sigma-Aldrich (Milwaukee, WI. USA). The chromogenic substrate, 3, 3´, 5, 5´-tetramethylbenzidine (TMB) was obtained from Dojindo (Osaka, Japan). Anti-influenza A virus HA (H1) antibody [B219M] (ab661189, Lot: GR40088-11) was purchased from Abcam Inc. (Cambridge, UK). Recombinant influenza virus A (New Caledonia/20/1999) (H1N1) (Cat No.: 11683-V08H) and anti-H3(H3N2) antibody HA MAb (Lot: HB04N0160) were purchased from Sino Biological Inc. (Beijing, China). Clinically isolated influenza virus A/Yokohama/110/2009 (H3N2) was kindly provided by Dr. C. Kawakami of the Yokohama City Institute of Health, Japan and was used for confirming the versatility of the assay system. All experiments were carried out using high purity deionized (DI) water (> 18 MΩ).

Synthesis of (+)Au NPs

The (+)Au NPs were prepared according to the published protocol (Jv et al., 2010). Briefly, a cysteamine solution (400 μL, 213 mM) was added to 40 mL of 1.42 mM $HAuCl_4$ solution. After stirring for 20 min at 25°C, 10 μL of 10 mM $NaBH_4$ solution was added, and the mixture was vigorously stirred for 10 min at 25°C in the dark. Then, the mixture was further stirred for 15 min, and the resulting wine-red solution was stored at 4°C until further use.

Characterization of (+)Au NPs

UV/vis absorption measurements were carried out using a filter-based multimode microplate reader (Infinite® F500, TECAN, Ltd, Männedorf, Switzerland). Surface

charges were measured with the Zetasizer (Nano-ZS, Malvern, UK). Transmission electron microscopy (TEM) images were generated using TEM JEM-2100F (JEOL, Ltd., Tokyo, Japan) operated at 100 kV. The concentration of the Au NPs was calculated based on Haiss's method (Haiss et al., 2007).

Conjugation of (+)Au NPs with Antibody

After the supernatant was separated by an ultracentrifuge (Kubota 6200, Tokyo, Japan) at 5,000 rpm for 30 min, the (+)Au NPs were dispersed in MilliQ water. Then, 1 mL of synthesized (+)Au NPs solution and 1 μL of HA antibody (Ab66189) (final concentration of 5 ng mL^{-1}) were incubated for 30 min and maintained at 4°C for 24 h. At this stage, the NPs were conjugated with the antibody through electrostatic interactions. The conjugated (+)Au NPs-antibodies were separated from their unconjugated or nonspecific binding partners through centrifugation (5,000 rpm, 30 min) and redispersed in 1 mL of Milli-Q water. To confirm antibody binding to (+)Au NPs, the samples were blocked with 100 μL of 2% BSA for 2 h at 25°C. One ng mL^{-1} anti-mouse IgG-HRP (Santa Cruz Biotechnology, CA) was added to each sample. After incubation at 25°C for 1 h, the samples were washed 3 times with phosphate buffered saline (PBS) solution. HRP was developed with 100 μL TMB substrate solution (10 μg mL^{-1} TMB, 10% H_2O_2 in 100 mM NaOAc, pH 6.0) for 5–30 min at 25°C. A blue color solution developed at this stage. The reaction was stopped by adding 100 μL of 10% H_2SO_4. The solution then became yellow in color, and its absorbance was read at 450 nm using a microplate reader (Model 680, Bio-Rad, Hercules, CA).

Detection of Influenza Viruses

Virus stock solution (influenza virus A (New Caledonia/20/1999) (H1N1)) was diluted

serially with PBS (pH 7.5) to perform sensing experiments. Virus solution (100 μL) was then added to each well of a 96 well microtiter plate (polystyrene, flat bottom, nonsterile, Becton Dickinson Labware, NJ) and incubated overnight at 4°C to allow adsorption of the virus to the plates. The plates were then rinsed with PBS (pH 7.5) and blocked with 100 μL of 2% skim milk for 2 h at 25°C. One ng mL^{-1} of antibody conjugated (+)Au NPs was added to the pre-adsorbed wells, and the plates were incubated for 1 h at 25°C. BSA (100 μL, 1 ng mL^{-1}) and influenza A (H3N2) virus (100 μL, 1 μg mL^{-1}) were used as a negative control and to demonstrate selectivity in this experiment, respectively. After washing three times, 100 μL of TMB and H_2O_2 (5 nM) mixture solution was added to each of the wells. The microplate was then incubated for 1 min at 25°C. At the last stage, 100 μL of 10% H_2SO_4 was added to each of the wells as a stopping reagent. The absorbance of the color was read at 655 nm using a plate reader (Model 680, Bio-Rad, Hercules, CA). Based on the absorbance values at different concentrations of influenza virus A (New Caledonia/20/1999) (H1N1), a dose-dependent curve was constructed. The same assay platform was applied to detect influenza virus A/Yokohama/110/2009 (H3N2) using anti-HA (H3N2) Ab-bioconjugated (+)Au NPs. To investigate the usability of the proposed detection method, a series of different concentrations of H3N2 viruses were prepared in the human serum and used for colorimetric detection. The limit of detection (LOD) was calculated according to the standard deviation method with little modification (Apostol et al., 2009). The details information of LOD calculation was given in supporting documents.

Acknowledgements

We thank Dr. Chiharu Kawakami of the Yokohama City Institute of Health, Japan, for providing influenza virus A/Yokohama/110/2009 (H3N2). This work was partially supported by the Promotion of Nanobio-Technology Research to support Aging and Welfare Society from the Ministry of Education, Culture, Sports, Science and Technology, Japan and by the International Research & Development Program of the National Research Foundation of Korea (NRF-2014K2A2A4001081). No additional external funding was received for this study.

References

Ahmed SR, Hossain M, Park JY, Kim SH, Lee D, Suzuki T, Lee J, Park EY. 2014. Metal enhanced fluorescence on nanoporous gold leaf-based assay platform for virus detection. Biosens Bioelectron 58: 33–39.

Apostol I, Miller KJ, Ratto J, Kelner DN.2009. Comparison of different approaches for evaluation of the detection and quantitation limits of a purity method: A case study using a capillary isoelectrofocusing method for a monoclonal antibody. Anal Biochem 385 :101–106.

Bonanni A, Pividori MI, del Valle M. 2010. Impedimetric detection of influenza A(H1N1) DNA sequence using carbon nanotubes platform and gold nanoparticles amplification. Analyst 135: 1765–1772.

Dong Yl, Zhang Hg, Rahman ZU, Su L, Chen Xj, Hu J, Chen Xg. 2012. Graphene oxide-Fe_3O_4 magnetic nanocomposites with peroxidase-like activity for colorimetric detection of glucose. Nanoscale 4: 3969–3976.

Gao Z, Xu M, Hou L, Chen G, Tang D. 2013. Magnetic bead-based reverse colorimetric immunoassay strategy for sensing biomolecules. Anal Chem 85: 6945–6952.

Gao Z, Xu M, Hou L, Chen G, Tang D. 2013. Irregular-shaped platinum nanoparticles as peroxidase mimics for highly efficient colorimetric immunoassay. Anal Chimica Acta 776: 79–86.

GaoZ, Hou L, Xu M, Tang D. 2014. Enhanced colorimetric immunoassay accompanying with enzyme cascade amplification strategy for ultrasensitive detection of low-abundance protein. Sci Rep 4:3966.

Gubala V, Harris LF, Ricco AJ, Tan MX, Williams DE. 2012. Point of care diagnostics: Status and future. Anal Chem 84: 487–515.

Haiss W, Thanh NTK, Aveyard J, Fernig DG. 2007. Determination of size and concentration of gold nanoparticles from UV-Vis spectra. Anal Chem 79: 4215-5221.

Hossain SMZ, Brennan JD. 2011. β-Galactosidase-Based colorimetric paper sensor for determination of heavy metals. Anal Chem 83: 8772-8778.

Jana NR, Gearheart L, Murphy CJ. 2001. Seeding Growth for Size Control of 5−40 nm Diameter Gold Nanoparticles. Langmuir 17: 6782-6786.

Jiang W, Wang Z, Beier RC, Jiang H, Wu Y, Shen J. 2013. Simultaneous determination of 13 fluoroquinolone and 22 sulfonamide residues in milk by a dual-colorimetric enzyme-linked immunosorbent assay. Anal Chem 85: 1995–1999.

Jv Y, Li B, Cao R. 2010. Positively-charged gold nanoparticles as peroxidiase mimic and their application in hydrogen peroxide and glucose detection. Chem Commun 46: 8017–8019.

Khavan-Tafti H, Binger DG, Blackwood JJ, Chen Y, Creager RS, de Silva R, Eickholt R A, Gaibor JE, Handley RS, Kapsner KP, Lopac SK, Mazelis ME, McLernon TL, Mendoza JD, Odegaard BH, Reddy SG, Salvati M, Schoenfelner BA, Shapir N, Shelly KR, Todtleben JC, Wang G, Xie WA. 2013. Homogeneous chemiluminescent

immunoassay method. J Am Chem Soc135: 4191–4194.

Lee BW, Bey RF, Baarsch MJ, Simonson RR. 1993. ELISA method for detection of influenza a infection in swine. J Vet Diagn Invest 5: 510–515.

Lekcharoensuk P, Lager KM, Vemulapalli R, Woodruff M, Vincent AL, Richt Jr A. 2006. Novel swine influenza virus subtype H3N1, United States. Emerg Infect Dis 12: 787–794.

Lin H, Liu Y, Huo J, Zhang A, Pan Y, Bai H, Jiao Z, Fang T, Wang X, Cai Y, Wang Q, Zhang Y, Qian X. 2013. Modified enzyme-linked immunosorbent assay strategy using graphene oxide sheets and gold nanoparticles functionalized with different antibody types. Anal Chem 85: 6228–6232.

Malashikhina N, Garai-Ibabe G, Pavlov V. 2013. Unconventional application of conventional enzymatic substrate: first fluorogenic immunoassay based on enzymatic formation of quantum dots. Anal Chem 85: 6866–6870.

Munge BS, Coffey AL, Doucette JM, Somba BK, Malhotra R, Patel V, Gutkind JS, Rusling JF. 2011. Nanostructured immunosensor for attomolar detection of cancer biomarker interleukin-8 using massively labeled superparamagnetic particles. Angew Chem Int Ed 50: 7915–7918.

Nguyen HH, Park J, Kang S, Kim M. 2015. Surface Plasmon Resonance: A Versatile Technique for Biosensor Applications. Sensors 15: 10481-10510.

Nidzworski D, Pranszke P, Grudniewska M, Król E, Gromadzka B. 2014. Universal biosensor for detection of influenza virus. Biosensors and Bioelectronics 59: 239–242.

Rodríguez-Lorenzo L, de la Rica R, Álvarez-Puebla R.A, Liz-Marzán LM, Stevens MM. 2012. Plasmonic nanosensors with inverse sensitivity by means of enzyme-guided

crystal growth. Nat Mater 11: 604–607.

Su L, Feng J, Zhou X, Ren C, Li H, Chen X. 2012. Colorimetric detection of urine glucose based $Znfe_2O_4$ magnetic nanoparticles. Anal Chem 84: 5753–5758.

Figure Legends

Figure 1. Schematic of virus detection using a peroxidase-mimic enzymatic reaction of gold nanoparticles and nanoparticle characterization. (A) Schematic of virus detection using (+)Au NPs: (a) viruses were deposited on a polystyrene 96-well plate; (b) antibody-conjugated (+)Au NPs were bound with virus through an antibody-antigen reaction, and unbound (+)Au NPs were washed out; (c) TMB-H_2O_2 was added, and (d) rapid color changes due to peroxidase activity of (+)Au NPs were noted; (B) and (C) absorbance spectrum and electron microscopic image of (+)Au NPs, respectively.

Figure 2. Catalytic activity of (+)Au NPs with HRP and TMB-H_2O_2. (A) ELISA results for anti-HA (H1N1) (Ab 66189) binding with (+)Au NPs; (B) A comparison study of catalytic activity towards TMB-H_2O_2.

Figure 3. Specificity and sensitivity of virus detection using catalytic activity of (+)Au NPs with TMB-H_2O_2. (A) Absorbance spectra of different mixing components in the presence of influenza virus A/New Caledonia/20/1999 (H1N1): a) target viruses/HA (Ab 66189)-conjugated (+)Au NPs/TMB-H_2O_2, b) target virus/ anti H3N2 MAb antibody-conjugated (+)Au NPs/TMB-H_2O_2, c) target virus/HA (Ab 66189)-conjugated (+)Au NPs/H_2O_2, and d) target virus/HA (Ab 66189)-conjugated (+)Au NPs/TMB. (B) Linearity of absorbance intensity corresponding to the influenza virus A/New Caledonia/20/1999(H1N1)

concentration. BSA was used as a negative control; H3N2 denotes influenza virus A/Yokohama/110/2009 (H3N2), which was used to assess detection specificity.

Figure 4. Detection and sensitivity comparison studies of clinically isolated virus sample. (A) ELISA results for anti-H3 HA MAb specificity for influenza virus A/Yokohama/110/2009 (H3N2), where HA (Ab 66189) and BSA were compared, and the binding affinity of anti-H3 antibody for (+)Au NPs using ELISA; (B) Absorbance versus influenza virus A/Yokohama/110/2009 (H3N2) concentration. BSA was used as a negative control; H1N1 denotes influenza virus A/New Caledonia/20/1999(H1N1), which was used for testing specificity; (C) Absorbance versus influenza virus A/Yokohama/110/2009 (H3N2) concentration using conventional ELISA; (D) Detection of influenza H3N2 virus in human serum.

Figure 1, Ahmed et al.

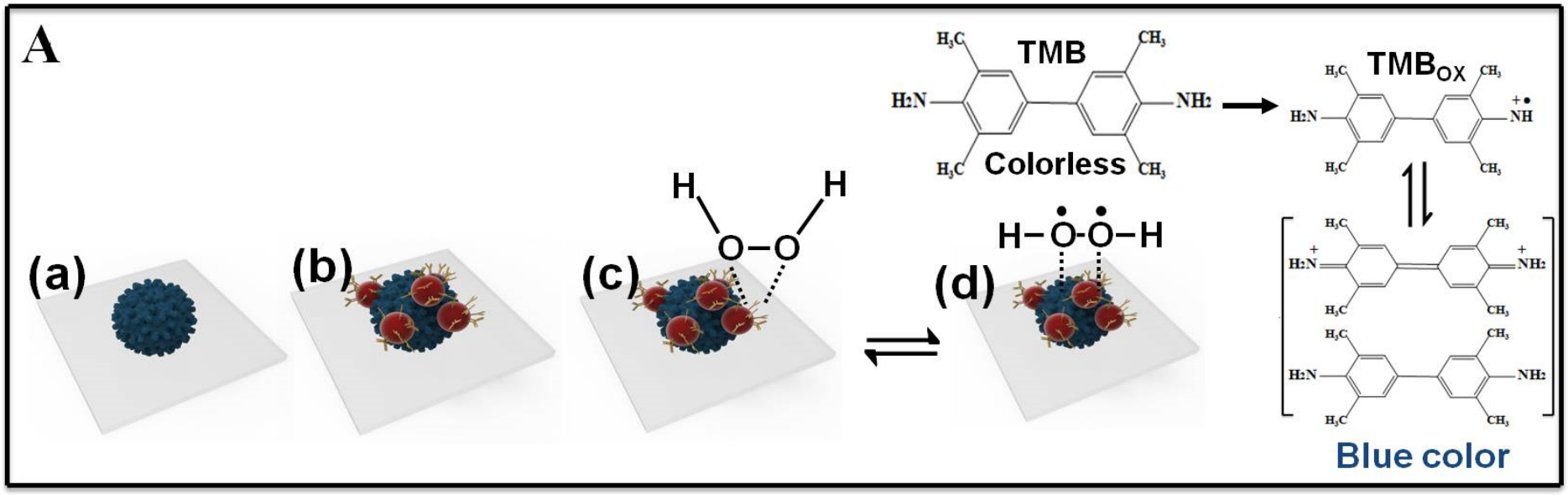

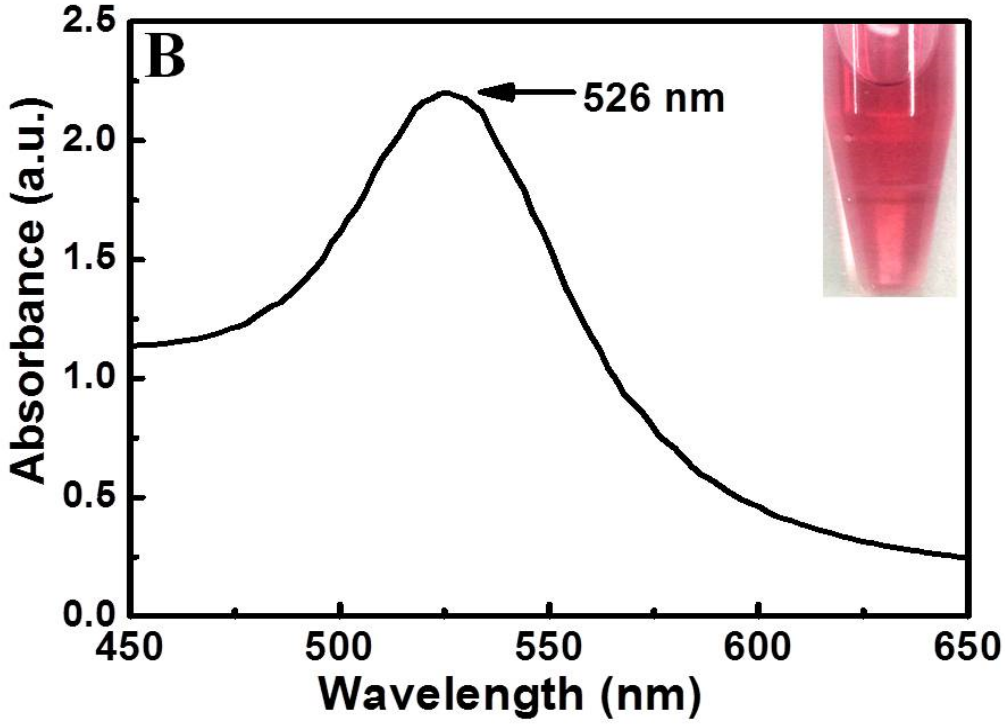

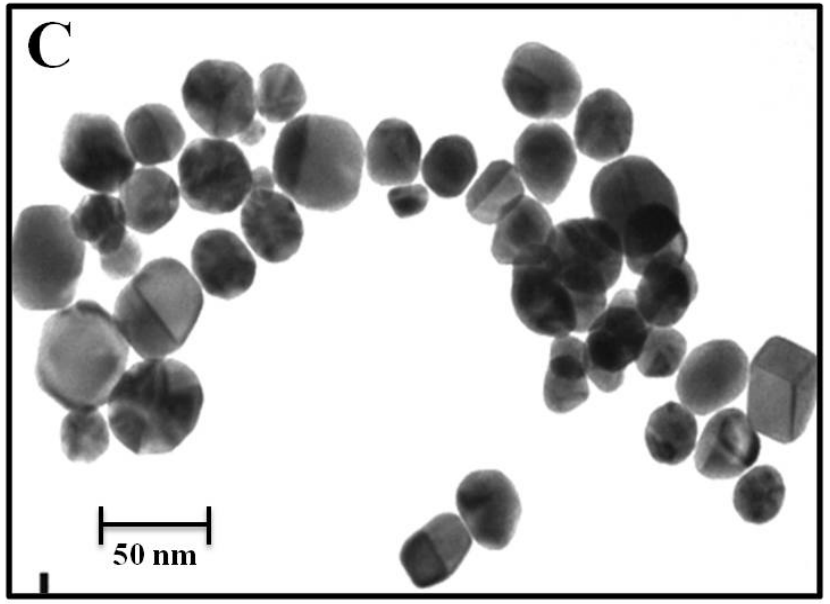

Figure 2, Ahmed et al.

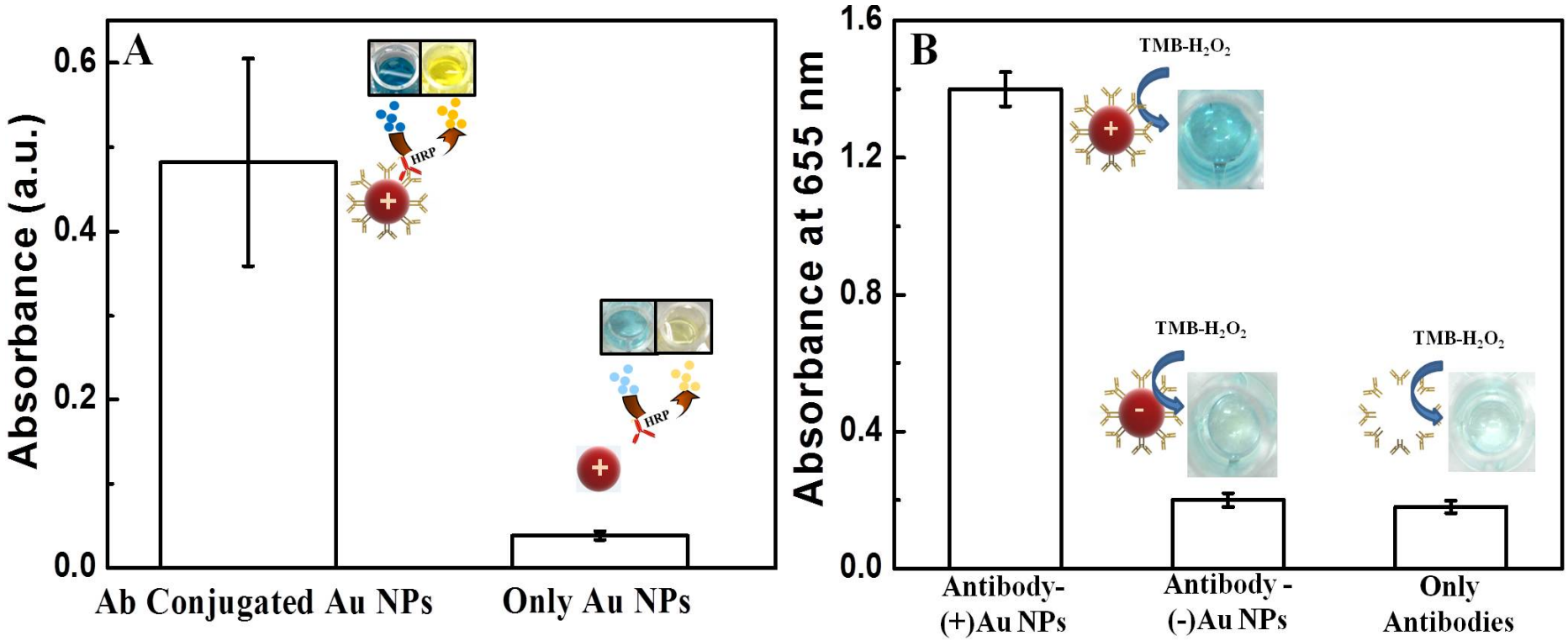

Figure 3, Ahmed et al.

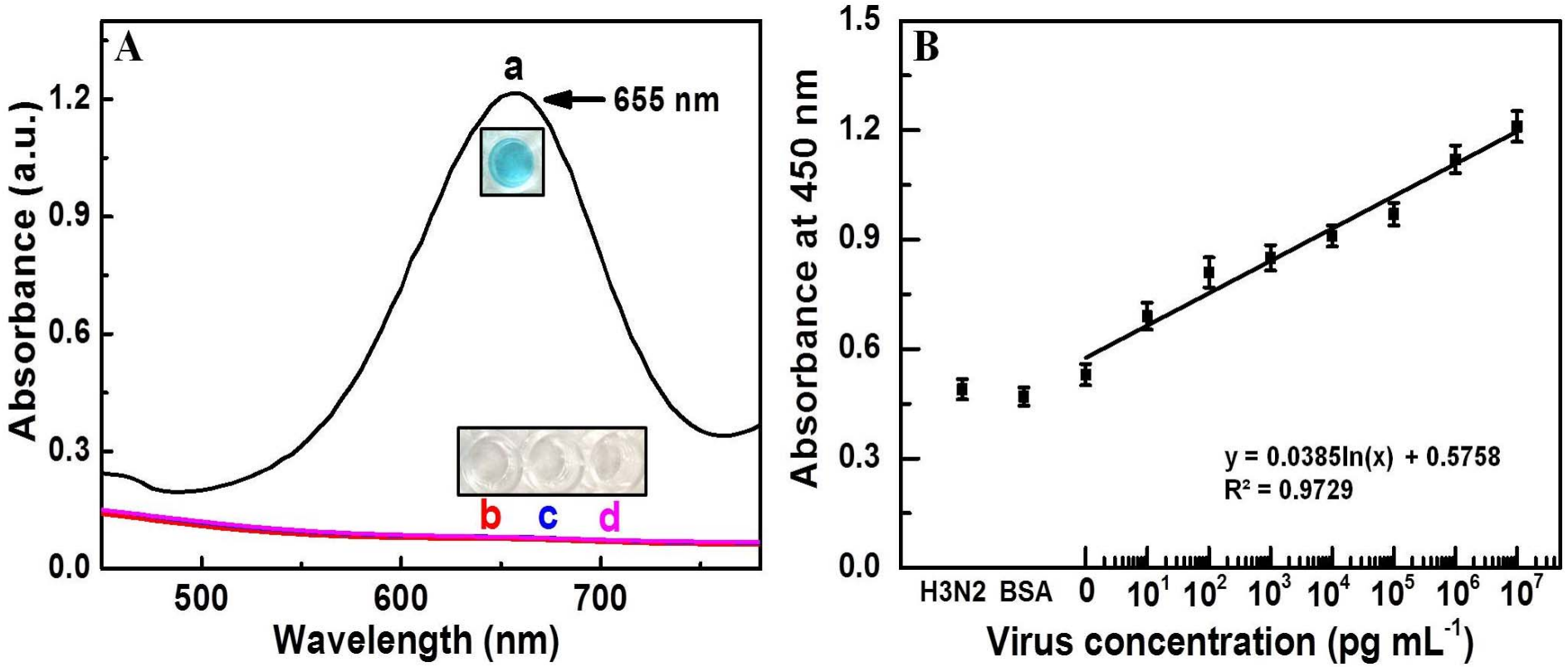

Figure 4, Ahmed et al.

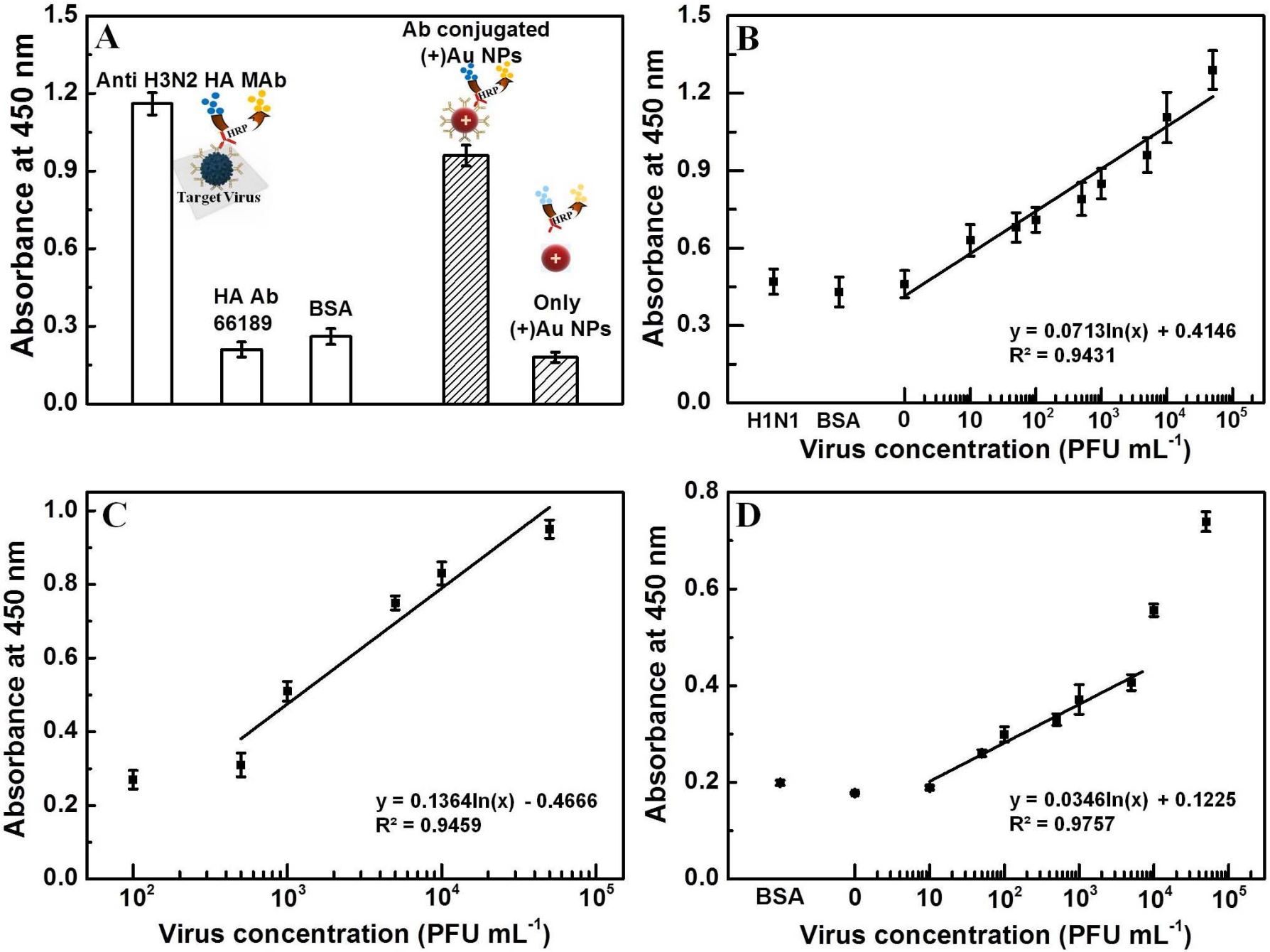

Supporting Information

Detection of Influenza Virus Using Peroxidase-mimic of Gold Nanoparticles

Syed Rahin Ahmed,[1] Jeonghyo Kim,[2] Tetsuro Suzuki,[3] Jaebeom Lee,[2,*] and Enoch Y. Park[1,4,*]

[1] Research Institute of Green Science and Technology, Shizuoka University, 836 Ohya Suruga- ku, Shizuoka, 422-8529, Japan.

[2] Department of Cogno-Mechatronics Engineering, Pusan National University, Busan, 609-735, Republic of Korea.

[3] Department of Infectious Diseases, Hamamatsu University School of Medicine, 1-20-1 Higashi-ku, Handa-yama, Hamamatsu 431-3192, Japan.

[4] Graduate School of Science and Technology, Shizuoka University, 836 Ohya Suruga-ku, Shizuoka 422-8529, Japan.

E-mail: rahin_sust@yahoo.com (SRA)
yaamako@gmail.com (JK)
tesuzuki@hama-med.ac.jp (TS)
jaebeom@pusan.ac.kr (JL)
park.enoch@shizuoka.ac.jp (EYP)

[*]Correspondence to: Enoch Y. Park; J. Lee

Table S1. Zeta Potential values of gold nanoparticles

Nanoparticles	Zeta potential (mV)	
	before conjugation with antibodies	after conjugation with antibodies
(+)Au NPs	+34.5	+29.3
(-)Au NPs	-35.9	-41.8

1. Characterization of negatively changed gold nanoparticles ((-)Au NPs).

Negatively changed gold nanoparticles ((-)Au NPs) are prepared as follow: briefly, 20 mL aqueous solution containing 2.5×10^{-4} M $HAuCl_4$ and 2.5×10^{-4} M trisodium citrate was mixed in a conical flask under continuously stirring. Next, 0.6 mL of ice-cold, freshly prepared 0.1 M $NaBH_4$ solution was added to the solution while stirring. The solution turned pink immediately after adding $NaBH_4$, indicating particle formation. Here, trisodium citrate serves as a both capping agent. The absorbance spectra and morphology synthesized (-)Au NPs are shown in Fig. S1.

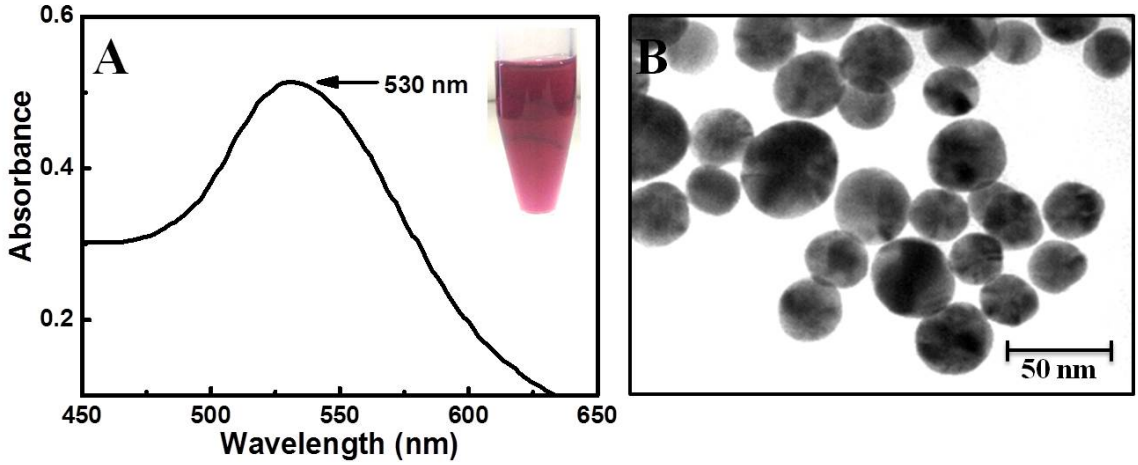

Figure S1. Characterization of (-)Au NPs. (A) Absorbance spectra of (-)Au NPs (inset: color of solution); (B) electron microscopic image of (-)Au NPs.

2. Conjugation of (-)Au NPs with anti-hemagglutinin (HA) antibodies (Ab66189) and its binding confirmation using EISA method

One ml of synthesized (-)Au NPs solution was mixed with EDC (4 mM) and NHS (10 mM) and incubated for 10 min, following by addition of 1 µL of HA Ab 66189 antibodies (final concentration of 5 ng mL^{-1}) and stirred at 4°C for 8 h. Finally, supernatant was removed, washed out unconjugated or nonspecific binding portion through centrifugation and dissolved in 1 mL MilliQ water. Antibody will bind with (-)Au NPs through amide bond. To check antibody binds with (-)Au NPs, samples were blocked with 100 µL of 2% BSA for 2 h at room temperature. One ng mL^{-1} anti-mouse IgG-HRP (Santa Cruz Biotechnology, CA, USA) was added to each sample. After incubation at room temperature for 1h, samples were washed 3 times with PBS buffer solution. HRP was developed with 100 µL TMBZ substrate solution (10 µg mL^{-1} TMB, 10% H_2O_2 in 100 mM NaOAc, pH 6.0) for 5–30 min at 25°C. A blue color solution developed at this stage. The reaction was stopped by adding 100 µL of 10% H_2SO_4. The solution then became yellow in color and the absorbance was read at 450 nm with a reference at 655 nm using a micro plate reader (Model 680, Bio-Rad, Hercules, CA, USA).

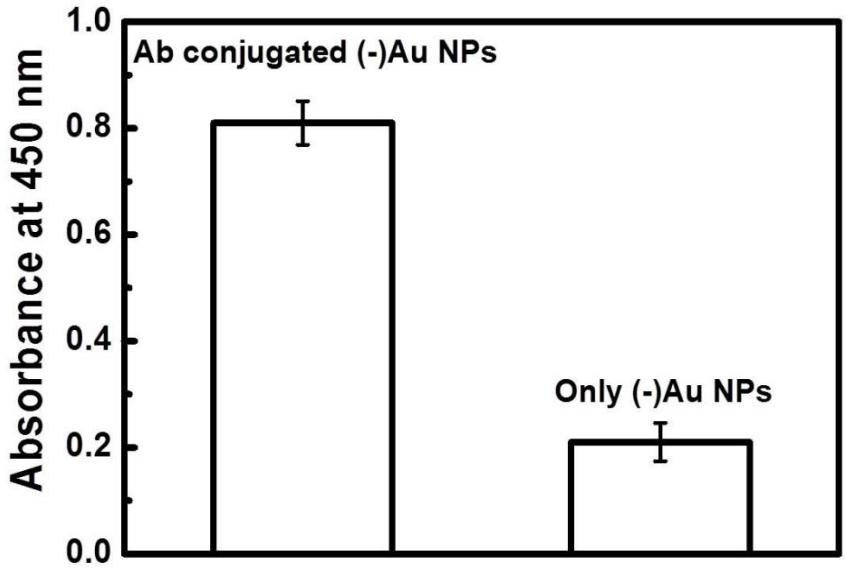

Figure S2. ELISA results of antibodies binding with (-)Au NPs.

3. Comparison study of catalytic activity between (+)Au NPs and HRP

To investigate the catalytic activity, a series of different concentrated solution of (+)Au NPs and HRP were prepared using MilliQ water and 1μL of each solution was mixed with 50 μL of TMB/H_2O_2 (5 nM) solution separately for 5 min in 96 well plate. After stopped the reaction with H_2SO_4, absorbance of TMB-derived oxidation products were measured using plate reader and shown in Figure S3. Catalytic activity increased with increasing concentration of both (+)Au NPs and HRP. However, in every cases, (+)Au NPs showed higher catalytic activity than HRP which might be applicable to increase the sensitivity of conventional ELISA method.

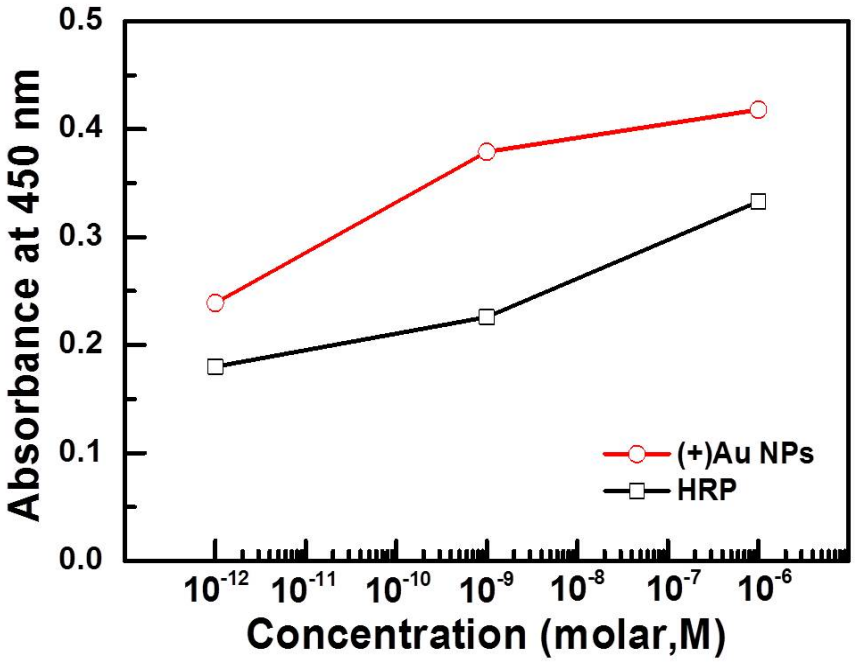

Figure S3. Comparison study of catalytic activity between (+)Au NPs and HRP.

4. Method of the determination of limit of detection:

The limit of detection (LOD) is calculated based on previously reported with little bit modification (Apostol et al., 2009). The absorbance intensity of blank samples was measured three times(n=3), and calculated the mean and standard deviation (SD_{blank}) values. In this work, it shows a logarithmic linear calibration curve for the detection of influenza virus, therefore a linear regression curve equation can be modified as following equation (1):

$$S = a + b \times \ln C \quad (1)$$

where S stands for the sensing signal (Absorbance at 450nm), C stands for the concentration of influenza virus, a is the intercept and b is the slope of the linear regression curve, i.e., sensitivity of sensing system. The signal of analyte at the lowest level of detection (Signal at limit of detection, S_{LOD}) is the production of the sensing system sensitivity (b) and the lowest concentration of analyte to be detected (C_{LOD}), this can be expressed as equation (2):

$$S_{LOD} = S_t - S_b = b \times \ln C_{LOD} \quad (2)$$

where S_t is total signal and S_b is background signal. The recognizable lowest signal, S_{LOD}, defined to be 3.3 times higher than the SD of the mean blank signal, SD_{blank}, as shown in equation (3):

$$S_{LOD} = b \times \ln C_{LOD} \geq 3.3\ SD_{blank} \quad (3)$$

The concentration of analyte at this lowest signal level (C_{LOD}) can be expressed as equation (4):

$$C_{LOD} = \mathrm{LOD} \geq e^{\frac{3.3 SD_{blank}}{b}} \quad (4)$$